JOURNAL OF MATERIALS SCIENCE 21 (1986) 3539–3547

High-temperature internal friction in polycrystalline Zircaloy-4

F. POVOLO
Departamento de Materiales, Comisión Nacional de Energía Atómica, Av. del Libertador 8250, 1429 Buenos Aires, and Facultad de Ciencias Exactas y Naturales, Departamento de Fisica, Universidad de Buenos Aires, Pabellón 2, Ciudad Universitaria, 1428 Buenos Aires, Argentina

B. J. MOLINAS
Departamento de Fisica, Universidad Nacional de Rosario, Instituto de Fisica Rosario, Av. Pellegrini 250, 2000 Rosario, Argentina

The high-temperature internal friction spectrum of polycrystalline Zircaloy-4 is investigated in detail, for a wide range of frequencies. Two internal friction maxima are observed. The lower-temperature peak is interpreted in terms of a relaxation mechanism produced by the sliding of particle-free grain boundaries. The higher-temperature peak is attributed to the sliding of boundaries blocked by small precipitates. Values for the activation enthalpy and the pre-exponential factor for diffusion along grain boundaries are given, and the viscosity coefficient associated with grain-boundary sliding is determined as a function of temperature.

1. Introduction

Povolo and Molinas [1] have reported recently some data on the high-temperature internal friction (HTIF) of polycrystalline zirconium and Zircaloy-4, obtained at low (of the order of 1 Hz) and at intermediate (of the order of 70 Hz) frequencies. The damping spectrum of pure zirconium, for annealed polycrystals, revealed one internal friction peak, P_1, both at low and at intermediate frequencies, which has been reported by several authors. This internal friction peak was found to be strongly dependent on the thermomechanical treatment given to the specimens and on the composition. The activation enthalpy, ΔH, and particularly the relaxation time, τ_0, vary according to different authors [2, 3] but a measurement of these parameters over a change in frequency of two orders of magnitude [1] and including the data of others [2, 3] leads to

$$\Delta H = (270 \pm 30)\,\mathrm{kJ\,mol^{-1}},$$
$$\tau_0 = 1.5 \times 10^{-(18\pm2)}\,\mathrm{sec} \quad (1)$$

These are the most reliable values for the activation enthalpy and the relaxation time for Peak P_1 in annealed zirconium polycrystals.

Two peaks have been observed, at least at low frequencies, on the HTIF spectrum of Zircaloy-4. Values for the activation enthalpy and the relaxation time similar to those for P_1 were observed for the lower-temperature peak, P'_1. It was not possible to measure the characteristic of Peak P'_2, occurring at higher temperatures, due to the fact that the peak is masked by the high-temperature background at intermediate frequencies and it was only resolved at low frequencies. Peaks P'_1 and P_1 were tentatively interpreted by us [1] as produced by dislocation movements occurring at the grain or subgrain boundaries, i.e. the peak present in pure zirconium and in the alloy is controlled by similar mechanisms. P'_2 was attributed to some precipitate at the grain boundary.

It is the purpose of this paper to present new data on the HTIF of annealed polycrystalline Zircaloy-4, obtained at frequencies between about 0.3 and 70 Hz. Due to the wide range of frequencies used it was possible to measure the characteristics of Peak P'_2 and to improve the accuracy of the values already reported for Peak P'_1.

Finally, the results will be discussed in terms of mechanisms involving grain-boundary sliding. The possible influence of impurities on the sliding rate will be also considered.

2. Experimental procedure

The specimens were prepared from nuclear grade Zircaloy-4, supplied by Teledyne Wah Chang (Albany, New York) as wires with 2 mm diameter. The chemical composition supplied by the manufacturer is given in Table I.

Two types of pendulum, working in a high vacuum, were used for the internal friction measurements:

(a) A low-frequency inverted torsion pendulum (Kê's pendulum) with a frequency between about 0.3 and 10 Hz. The internal friction was obtained from the decay of the oscillations, registered by means of a photodiode on the screen of an oscilloscope with memory and on a recorder. Typically, maximum strain amplitudes between 3×10^{-5} and 8×10^{-6} were obtained on the surface of the specimens during free decay.

(b) An automatic pendulum working at intermediate frequencies, of the order of 70 Hz. This

0022–2461/86 $03.00 + .12

TABLE I Properties of Zircaloy-4

Composition (wt %)	
Sn	1.41
Fe	0.19
Cr	0.1
Zr	balance
Main impurities (p.p.m. by mass)	
C	135
Hf	60
N	45
Al	35
Ni	19
Si	28
Ti	18
W	< 25
O	980

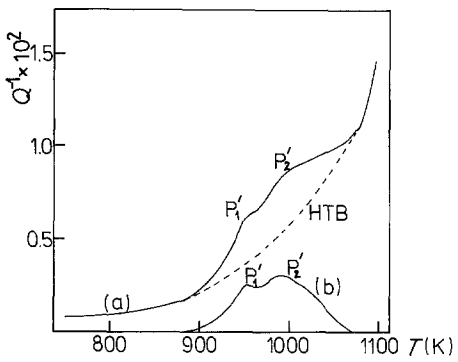

Figure 1 (a) HTIF spectrum of polycrystalline Zircaloy-4 at intermediate frequencies. (b) P'_1/P'_2 complex obtained after subtracting out the background (HTB).

equipment allows measurements of the damping at constant maximum strain amplitude and the internal friction against temperature is recorded automatically. In this type of pendulum, the internal friction is recorded in terms of the energy required to maintain a given oscillation amplitude. Since this energy is proportional to f^{-2}, where f is the oscillation frequency, the recorded internal friction against temperature can be distorted if the oscillation frequency changes considerably with the temperature. A special feature of the pendulum used is that this effect is corrected automatically so that an undistorted recording of the damping against temperature is obtained. The details of the pendulum are given elsewhere [4].

Finally, two types of specimen were used for the measurements: the as-received 2 mm diameter wires at intermediate frequencies and 1 mm diameter wires at low frequencies, obtained by chemically etching the as-received material.

3. Results

The average grain size of the as-received material was of the order of 16 μm (measured according to ASTM E112 standards). Prior to the internal friction experiments, all the specimens were annealed, during 1 to 2 h in a high vacuum, at temperatures of the order of 1023 K. The precise annealing treatment and the average grain size, l_i, after the annealing treatment and l_f, after the internal friction measurements, are given in the third and fifth column of Table II, respectively. The fourth column gives the oscillation frequency of each specimen at room temperature.

After the annealing treatment and unless otherwise specifically stated, the specimens were located into the pendulum and heated at a rate of 320 K h^{-1} up to 1073 K. After holding the specimen for 30 min at this temperature, the internal friction curve was measured on cooling at an average rate of 80 K h^{-1}.

TABLE II Characteristics of Zircaloy-4 specimens measured at different frequencies

Specimen	Annealing treatment	l_i (μm)	f (Hz)	l_f (μm)	ΔH_{HTB} (kJ mol^{-1})
1	1 h, 1013 K	19	93	21	88
2	2 h, 1023 K	25	11.5	26	88
3	2 h, 1023 K	25	2.3	26	80
4	1 h, 1023 K	27	0.9	37	84
5	2 h, 1023 K	25	0.38	29	80

As described earlier [1], the HTIF spectrum of Zircaloy-4 consists of two peaks, P'_1 and P'_2, and a high-temperature background (HTB). This is illustrated by Curve (a) of Fig. 1 for a specimen measured at intermediate frequencies, with the automatic pendulum. This specimen, not listed in Table II, had been subjected to a "grain growth" treatment [1] and the average grain size, before the internal friction measurement, was of the order of 42 μm. The peaks can be subtracted from the total damping by assuming an exponential increase of the HTB with temperature [1, 5], i.e. the internal friction was plotted as $\log Q^{-1}$ against T^{-1} and a straight line was drawn through the data below and above the peaks. This is shown by the increasing broken curve of Fig. 1. The peaks obtained after subtracting the HTB are given by Curve (b) of Fig. 1. It is clear that it is difficult to resolve each individual peak for the data obtained at intermediate frequencies. The situation improves at lower frequencies, as illustrated by the curves shown in Fig. 2 obtained for Specimens 3 and 4 of Table II. The HTB has been subtracted out by using the procedure already described.

Table III gives the different parameters for Peaks P'_1 and P'_2 obtained at various oscillation frequencies, for the specimens listed in Table II. T_p is the peak temperature, f_p is the frequency at the peak, Q_p^{-1} is the height of the peak and $\Delta(T^{-1})$ the peak width at half maximum. In Table III, the first row for each specimen gives the data for Peak P'_1 and the second row

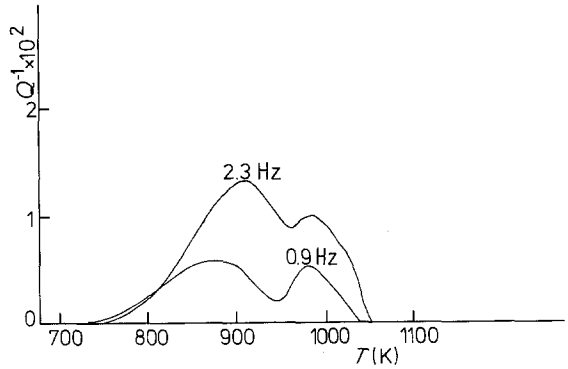

Figure 2 P'_1/P'_2 complex at low frequencies.

TABLE III Characteristics of Peaks P'_1 and P'_2 measured on specimens listed in Table II

Specimen		f_p(Hz)	T_p(K)	$Q_m^{-1} \times 10^{-2}$	$\Delta(T^{-1})$ ($K^{-1} \times 10^{-4}$)	β	$\Delta_j \times 10^{-2}$
1	P'_1	70	982	1.8	1.4	2.8	7.2
	P'_2	–	–	–	–	–	–
2	P'_1	8.54	932	2.2	1.7	3.5	10.7
	P'_2	–	–	–	–	–	–
3	P'_1	1.82	907	1.3	1.2	2.1	4.6
	P'_2	1.68	983	1.0	0.97	1.44	2.8
4	P'_1	0.632	876	0.58	1.5	3.1	2.6
	P'_2	0.582	977	0.52	0.62	0	0.52
5	P'_1	0.306	867	1.5	1.0	1.7	4.3
	P'_2	0.283	953	1.9	1.1	1.8	5.8

those for P'_2, respectively. Peak P'_2 could not be reasonably resolved at the higher frequencies so that no data are reported. It must be pointed out that the individual peaks were resolved from plots similar to those given in Fig. 2 and by assuming that each peak is symmetric about the maximum.

On assuming [6] that the maximum occurs at

$$2\pi f_p \tau = 1 \tag{2}$$

and

$$\tau = \tau_0 \exp(\Delta H/kT) \tag{3}$$

then combining Equations 2 and 3 leads to

$$\ln f_p = -\ln(2\pi\tau_0) - (\Delta H/kT_p) \tag{4}$$

According to Equation 4 a plot of $\ln f_p$ against T_p^{-1} should give a straight line of slope $(\Delta H/k)$ and intercept $-\ln(2\pi\tau_0)$. The data of Table II are plotted according to Equation 4 in Fig. 3. ΔH and τ_0 obtained from the slopes and the intercepts of the straight lines are indicated in the same figure. The values obtained for P'_1 are similar to those reported earlier [1] and to the values obtained for Peak P_1 in pure zirconium, as shown by Equation 1. A higher value for ΔH and a lower value for τ_0 is found for Peak P'_2.

As already pointed out [1], an important difference between the HTIF or zirconium and Zircaloy-4 is that the damping of the alloy is fairly reproducible either on heating or on cooling. This is not the case for zirconium, where hysteresis phenomena are observed [7, 8] and the grain size is changing during the internal friction measurements. In fact, as shown by Table II, where l_f indicates the average grain size of the specimens after the internal friction experiments, the grain size does not change substantially from the value, l_i, obtained after the annealing treatment. Furthermore, Peaks P'_1 and P'_2 do not vary appreciably on changing the heating or the cooling rate, or even when the specimen is heated above the α–β transition temperature (of the order of 1073 K). This is illustrated in Fig. 4, for data obtained at intermediate frequencies on the same specimen as for Fig. 1. Curve (a) was measured at a heating rate of 320 K h^{-1} up to point P, above the phase transition; Curve (b) on cooling at the

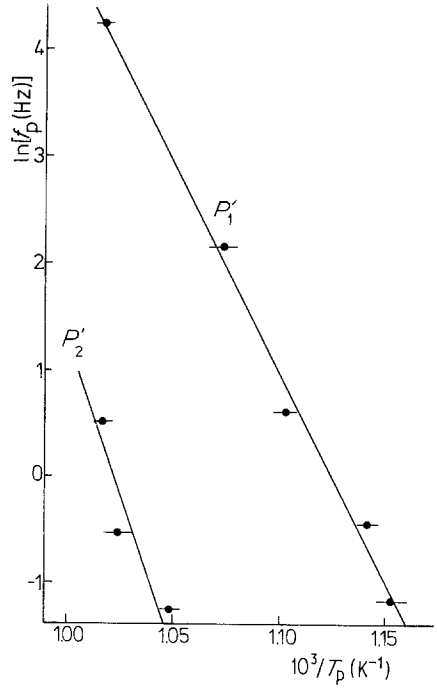

Figure 3 Plot of the data given in Table III according to Equation 4. The pre-exponential factors and the activation enthalpies are as follows. For P'_1, $\Delta H = 330 \pm 17\,\mathrm{kJ\,mol^{-1}}$, $\tau_0 = 6.9 \times 10^{-(21\pm1)}$ sec, for P'_2, $\Delta H = 395 \pm 100\,\mathrm{kJ\,mol^{-1}}$, $\tau_0 = 1.28 \times 10^{-(22\pm3)}$ sec.

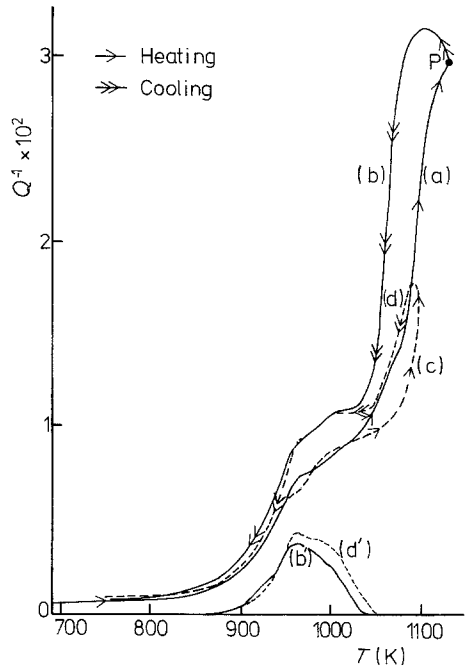

Figure 4 Hysteresis observed on the HTIF of Zircaloy-4, (a) measured on heating at a rate of 320 K h^{-1} and (b) measured on a subsequent cooling from point P at the same rate. (c) Obtained on a subsequent heating at a rate of 80 K h^{-1} and (d) on cooling at the same rate. Curves (b') and (d') were obtained from curves (b) and (d), respectively, after subtracting the HTB.

same rate. It is seen how the internal friction peak due to the $\alpha-\beta$ transition develops. Curve (c) was obtained during a subsequent heating at 80 K h^{-1} and Curve (d) on cooling at the same rate. It is clear that only the HTB varies considerably during successive runs and only minor changes are produced in the $P'_1-P'_2$ complex. This is illustrated by Curves (b′) and (d′), obtained from Curves (b) and (d), respectively, after subtracting the HTB.

Finally, the last column of Table II gives the values for the apparent activation enthalpy for the HTB, ΔH_{HTB}, obtained in the different specimens from a linear plot of $\log Q^{-1}$ against T^{-1} below and above the peaks. As shown before [1], ΔH_{HTB} depends on the grain size and the values given in Table II fall within those given by the plot of ΔH_{HTB} against l, where l is the grain size (see Fig. 9 of [1]). ΔH_{HTB} is the same for all the specimens listed in Table II, within the experimental error (of the order of 10%).

4. Discussion

Povolo and Molinas [8] have recently studied the HTIF of polycrystalline zirconium in detail, and both the hysteresis effects present and the two internal friction maxima were explained by a relaxation mechanism associated with grain-boundary sliding and segregation of impurities to the grain boundaries. The lower-temperature peak was attributed to the sliding of the particle-free boundaries and the high-temperature peak to the sliding of the particle-bearing boundaries. A similar mechanism should also control the HTIF of Zircaloy-4. In fact, Sun and Kê [9] have proposed a theory to describe the internal friction produced by relaxation processes occurring in the grain boundaries. The theory is based on a continous-distribution dislocation model of high-angle boundaries, and the internal friction is given by

$$Q^{-1} = \frac{\pi(1-\nu)}{2}(4p - C)\frac{q}{p^2} \quad (5)$$

where

$$C = \pi(1-\nu)\, l\omega\eta/\mu d \quad (6)$$

$$2p + \frac{1}{(1+p^2)^{1/2}} \ln \frac{1 + p^2 + p(1+p^2)^{1/2}}{1 + p^2 - p(1+p^2)^{1/2}} = C \quad (7)$$

$$\frac{(1+p^2)^{3/2}}{\pi + pC(1+p^2)^{1/2}} = q \quad (8)$$

ν is Poisson's ratio, l the grain size, μ the shear modulus, d the width of the grain boundary, $\omega = 2\pi f$ the angular frequency of the applied stress and η the assumed viscosity coefficient associated with grain-boundary sliding. p and q are defined through the parameter C. Equation 5 describes a peak in a Q^{-1} against C plot with a maximum [9] given by

$$Q_m^{-1} = 0.293\pi\,(1-\nu)/2 \quad (9)$$

According to Sun and Kê [9] the grain-boundary viscosity is given by

$$\eta = \frac{kTd}{a\boldsymbol{b}D_{b0}} \exp\left(\frac{\Delta H_b}{kT}\right) \quad (10)$$

where $\boldsymbol{b}$ is the Burgers vector and $a \simeq \boldsymbol{b}$ is the average length of a segment of grain-boundary mobile dislocations [9] and

$$D_b = D_{b0} \exp(-\Delta H_b/kT) \quad (11)$$

is the diffusion coefficient along grain boundaries. On substituting Equation 10 into Equation 6 this leads to

$$C = 2\pi^2(1-\nu)\frac{lfkT}{a\boldsymbol{b}\mu D_{b0}} \exp\left(\frac{\Delta H_b}{kT}\right) \quad (12)$$

The peak described by Equation 5 is compared with a Debye-type peak in Fig. 5. The detailed analysis and the peak width at half maximum, when the internal friction is measured as a function of temperature, are given in Appendix A.

According to Equation 5 the maximum occurs at $C = 4.269$ (see Appendix A) and on introducing this value into Equation 12, taking logarithms and rearranging terms, this leads to

$$\ln\left(\frac{f_p T_p}{\mu}\right) = \ln \frac{4.269\, a\boldsymbol{b}D_{b0}}{2\pi^2 l(1-\nu)k} - \frac{\Delta H_b}{kT_p} \quad (13)$$

A plot of $\ln(f_p T_p/\mu)$ against T_p^{-1} should then give a straight line of slope $(\Delta H_b/k)$ and intercept $\ln[4.269\, a\boldsymbol{b}D_{b0}/2\pi^2(1-\nu)kl]$. Such a plot is shown in Fig. 6 for the data obtained from Peaks P'_1 and P'_2, using the f_p and T_p values given in Table II and

$$\mu = 35.5 - 0.0198(T - 273) \quad \text{GPa} \quad (14)$$

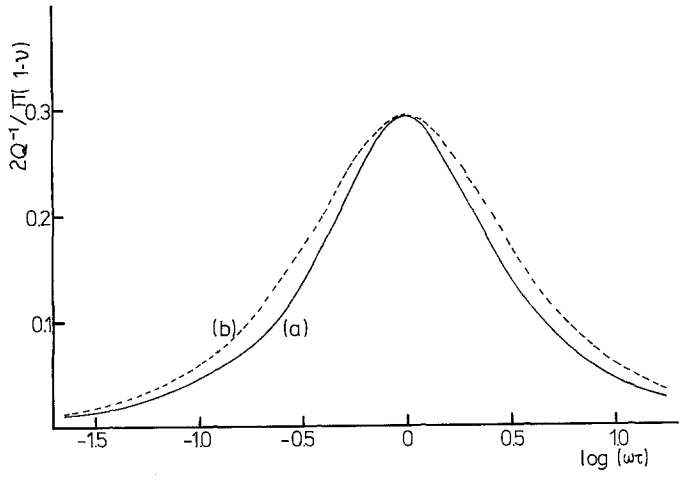

Figure 5 Comparison between the internal friction peak (a) described by Equation 5, and (b) a Debye peak.

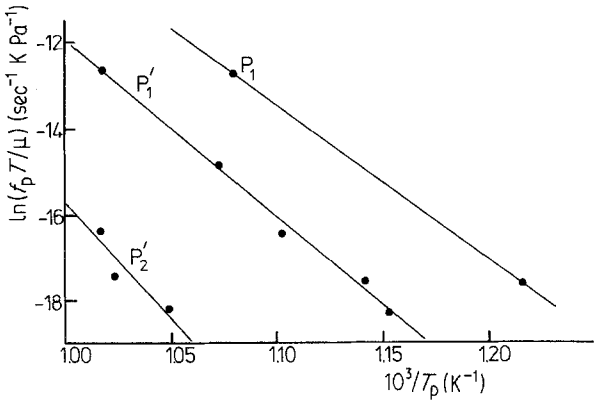

Figure 6 Plot of the data given in Table III according to Equation 13. The data reported for Peak P_1 in pure zirconium [1] have also been included.

as reported by Rosinger *et al.* [10]. Due to the uncertainties in the temperature dependence of v [11], this parameter has been taken as independent of temperature. l has been considered constant since the grain size changes only slightly, as shown in Table II. In any case, the straight lines shown in Fig. 6, both for P'_1 and for P'_2, lead to values for ΔH_b similar to those for ΔH given in Fig. 3, since the exponential term is dominant in Equation 12. The data for Peak P_1 in pure zirconium, reported at low and at intermediate frequencies [1], have been also included in Fig. 6 for comparison.

It must be pointed out that the plot suggested by Equation 4, shown in Fig. 3 and generally used, is based on a Debye-type peak [6] which is associated with atomic jumps. In such a case τ_0 should be of the order of $\nu_D^{-1} \simeq 10^{13}$ Hz, where ν_D is the Debye frequency. As shown in Fig. 3, however, the experimental values for τ_0 are much smaller. The situation changes completely when the data are described by Equation 13, where the pre-exponential factor has a completely different interpretation. The values obtained for D_{b0}/l from the intercept of the straight lines shown in Fig. 6 and those for D_{b0}, on taking for l the measured grain size, $v = 0.3$ and $a = b = 3.23 \times 10^{-10}$ m, are given in Table IV. Furthermore, within the experimental error it can be assumed that ΔH_b has the same value for the three peaks, and since this parameter has been obtained for Peak P'_1 with the higher accuracy it will be assumed that $\Delta H_b = 330\,\text{kJ mol}^{-1}$ for the three peaks, as indicated in the last row of Table IV. The values given in the lower row for Peak P'_2 are obtained when it is assumed that the straight line for P'_2 of Fig. 6 is parallel to the straight line for P'_1. It is seen that large errors are involved in the determination of the parameters for Peak P'_2.

TABLE IV Pre-exponential factor and activation enthalpy for the diffusion coefficient along grain boundaries, obtained from the internal friction data for zirconium and Zircaloy-4

Peak	D_{b0}/l (m sec^{-1})	D_{b0} (m^2 sec^{-1})
P_1	6.6×10^7	5.9×10^3 ($l = 90\,\mu$m)
P'_1	2.4×10^9	7.2×10^4 ($l = 30\,\mu$m)
P'_2	1.6×10^{11}	4.8×10^6 ($l = 30\,\mu$m)
	7.9×10^6	2.4×10^2 ($l = 30\,\mu$m)

$\Delta H_b = 330\,\text{kJ mol}^{-1}$

If the internal friction peaks are to be interpreted within the model of Sun and Kê [9], an important parameter to be considered is the peak width at half maximum. The theoretical width can be calculated with Equation A7 from Appendix A and ΔH_b given in Table IV, which leads to $\Delta(T^{-1}) = 6.1 \times 10^{-5}\,\text{K}^{-1}$. As shown in Table III the experimental widths are, in general, much higher. It should be pointed out, however, that the theory assumes that all the grains are of the same size and have the same thickness. This is not actually the case and the grain sizes are distributed about a mean value. The distribution is different in different dimensions and the grain-size distribution is not log normal [12].

For the particular case of recrystallized zirconium Colin and Lehr [13] have shown that the distribution of the grains as a function of their mean diameter approximates closely the log-normal law, when the grains are divided into categories of which the limits form a geometric progression. Furthermore, even on assuming that the grain-size distribution is normal in $\ln l$ and that d is constant, it is difficult to incorporate the distribution into Equation 5. An estimate of the influence of the grain-size distribution on Q^{-1} can be made by using a procedure similar to the one proposed by Nowick and Berry [14]. It is shown in Appendix A that Equation 5 can be approximated by

$$Q^{-1} = 0.293\pi(1 - v)\,[\omega\tau/1 + \omega^2\tau^2] \quad (15)$$

with

$$\tau = \tau_0\, T \exp(\Delta H_b/kT) \quad (16)$$

and

$$\tau_0 = (1 - v)\,k\pi l/4.269\,\mu a b D_{b0} \quad (17)$$

A distribution in l then induces a distribution in τ. The formalism developed by Nowick and Berry can be applied to Equations 15 to 17 on assuming that the distribution is normal in $\ln l$ (log-normal distribution) and that a, b and D_{b0} are constants. Extending the procedure given by Nowick and Berry [14] to this case leads to

$$r_2(\beta) = \frac{(\Delta H_b/k)\,\Delta(T^{-1}) + \Delta \ln T}{2.635} \simeq \frac{\Delta H_b}{2.635\,k\Delta(T^{-1})} \quad (18)$$

$$Q_m^{-1} = f_2(0, \beta)\,\frac{\Delta_j}{1 + \frac{1}{2}\Delta_j} \quad (19)$$

where $r_2(\beta)$ and $f_2(0, \beta)$ are functions tabulated by Nowick and Berry [14] as a function of β. The latter is a parameter that measures the width of the Gaussian distribution ($\beta = 0$ means a single relaxation time) and Δ_j is the relaxation strength, i.e. twice the height of the peak corresponding to a single relaxation time equal to the average value. Equation 18 can be used to obtain $r_2(\beta)$ from the measured values for $\Delta(T^{-1})$ given in Table III. Once $r_2(\beta)$ is known, β can be obtained from the published tables of $r_2(\beta)$ against β [14]. Furthermore, Δ_j can be obtained by means of Equation 19, on using the measured Q_m^{-1} values given

in Table III and $f_2(0, \beta)$ obtained from the tabulated values as a function of β [14]. β and Δ_j obtained in this way for Peaks P'_1 and P'_2, for $\Delta H_b = 330\,kJ\,mol^{-1}$, are given by the last two columns of Table III. No clear dependence on temperature is found for the parameter β, and consequently the distribution is only in τ_0 and not in ΔH_b [14]. According to the Sun and Kê model [9] the internal friction maximum should be given by Equation 9, which on putting $v = 0.3$ gives

$$Q_m^{-1} \simeq 0.3 \qquad (20)$$

independent of the grain size. When the values given for Δ_j in Tables III are compared with the value given in Equation 20 it is seen that Δ_j is much smaller. It should be taken into account, however, that Δ_j is only an estimate due to the simplifications implied by Equations 15 to 17 and the various assumptions made by Nowick and Berry [14] in their treatment of the problem. In fact, it was assumed in the derivation of Equation 1 that all the grains have the same size. Furthermore, in the derivation of Equations 18 and 19, i.e. in the estimation of Δ_j, it was assumed that the grain-size distribution is log-normal, which might not be the case. There are also large experimental errors in the determination of the experimental width at half maximum, due to the fact that the peaks are small and must be subtracted out from the background. In the case of zirconium, where the peaks are much higher and much better defined over the background, the agreement between the calculated and the measured maxima is much better [8].

In summary, it is proposed that P'_1 (Peak P_1 in pure zirconium [8]) and P'_2 (Peak P_2 in pure ziconium [8]) are related to processes occurring at the grain boundaries. P'_1 is produced by the sliding of particle-free boundaries and P'_2 by the sliding of particle-bearing boundaries. In other words, P'_1 will be described by the Sun and Kê model for an orthodox grain-boundary peak, and P'_2 will be associated with a change in the intrinsic viscosity of the grain boundary due to the segregation of solutes along certain boundaries, as suggested by them [9].

The Sun and Kê model does not consider the interaction of particles with the grain boundaries. Mori *et al.* [15] have proposed recently a theory for grain-boundary sliding and the associated internal friction, including the blocking effect of second-phase particles. The authors did not make a detailed calculation of the internal friction peaks, but they have shown that the relaxation time for the sliding of the particle-bearing boundaries, τ, is given by

$$\tau^* = \frac{\tau}{1 + (\pi l r / 2\lambda^2)} \qquad (21)$$

where τ is the relaxation time for the sliding of the particle-free boundary, λ is the interparticle spacing and r is the average radius of the blocking particle. On assuming that τ^* is given by Equation 21 and taking into account Equations 16 and 17, it is easy to show that the ratio between the exponentials of the intercepts of the straight lines shown in Fig. 6 is equal to the ratio between D_{b0}/l, obtained for each peak (see Equation 13). In fact

$$\frac{\exp I_{P'_1}}{\exp I_{P'_2}} = \frac{(D_{b0}/l)_{P'_1}}{(D_{b0}/l)_{P'_2}} = 1 + \pi l r / 2\lambda^2 \qquad (22)$$

where I is the intercept of the straight lines shown in Fig. 6. On taking the values for D_{b0}/l given in Table IV (the lower row for P'_2), Equation 22 leads to

$$\lambda^2 / r = 1.6 \times 10^{-7} \quad m \qquad (23)$$

If r is the order of the limit of the resolution of an electron microscope, i.e. of the order of 10b, where b is the lattice parameter of zirconium, Equation 23 gives

$$\lambda = 70b \qquad (24)$$

which is a reasonable value. Unfortunately, there is no information in the literature about precipitation at grain boundaries in zirconium and zirconium alloys. In any case, the value given by Equation 24 should be considered only as an order of magnitude estimation, since several assumptions are involved in the theories considered and the complex structure of the grain boundaries is oversimplified. As shown in Appendix B, only small amounts of impurities are necessary to saturate the grain boundaries. Equation 18, for example, gives for oxygen in zirconium an impurity content of 4 p.p.m. by weight. Since a much lower content is needed to block grain-boundary sliding, it is clear that the effect of segregated impurities is important even in very pure metals. Furthermore, a segregation of impurities to grain boundaries would explain the fact that a peak similar to P'_2 is observed in pure zirconium, and also explain the grain-size dependence of the hysteresis observed in the HTIF of the pure metal. The details are given elsewhere [8].

Some comments should be made about the value for the diffusion coefficient along grain boundaries from the internal friction data. P'_1 (and P_1) is assumed to be generated by sliding of the particle-free boundaries (those free from particles giving rise to P'_2) and since the parameters for this peak have been determined with the greatest accuracy, it may be assumed that D_{b0} for Peak P'_1, given in Table II, represents the most reliable value for the pre-exponential factor of D_b. Then

$$D_b = 7.2 \times 10^4 \exp \frac{-330\,(kJ\,mol^{-1})}{kT} \quad m^2\,sec^{-1} \qquad (25)$$

It must be pointed out that this equation gives only an order of magnitude estimate for D_b, since l may be smaller than the actual grain size. In fact, ledges, protrusions and stable precipitates may act as obstructing sites for grain boundary sliding. ΔH_b is much higher than the activation enthalpy for self-diffusion in zirconium, which is of the order of $100\,kJ\,mol^{-1}$ [16, 17]. D_b obtained by internal friction techniques, however, has the meaning of a diffusion coefficient related to grain-boundary sliding and it is associated with an average viscosity. The values obtained for grain-boundary diffusion coefficients by means of other techniques (autoradiography, etc.) may have a

completely different significance. In any case, it is generally observed that both D_{b0} and ΔH_b depend strongly on the purity of the material [18]. Furthermore, the theories of Sun and Kê [9], Mori *et al.* [15] and Mosher and Raj [19] for the internal friction produced by grain-boundary sliding are similar in some aspects, except for some geometrical factors, in the sense that they use a continuous model description of grain boundaries. Within these models, the activation enthalpy is introduced via a diffusion coefficient along grain boundaries (Equation 11) and a grain-boundary viscosity is also introduced in terms of this diffusion coefficient.

Shvedov [20] has proposed a more discrete theory of grain-boundary relaxation, based on the movement of the segments of screw grain-boundary dislocations where the movement of these dislocations is controlled by the climbing of jogs and demands vacancy flow. In this model

$$Q_p = Q_b + Q_v \frac{l'}{L_0}\left(0.693 + \frac{5L_0}{8l'} - \frac{U_j - Q_v/4}{kT_p}\right) \quad (26)$$

where Q_p is the activation energy obtained from a shift of the internal friction peak with frequency, Q_v is the activation energy for volume self-diffusion, Q_b is the activation energy for boundary self-diffusion, L_0 is the length of a grain-boundary dislocation segment when relaxation is controlled only by boundary diffusion, U_j is the jog formation energy on the lattice dislocations and l' is the average spacing between jogs on the grain-boundary dislocations. With $Q_v = 100\,\mathrm{kJ\,mol^{-1}}$, $U_j = 22\,\mathrm{kJ\,mol^{-1}}$ [17], $Q_b = Q_v/2$, $Q_p = 330\,\mathrm{kJ\,mol^{-1}}$ and $T_p = 982\,\mathrm{K}$, as obtained for Specimen 1 and given in Table III, Equation 26 leads to

$$l'/L_0 \simeq 3 \quad (27)$$

Equation 27 implies that $L_0 < l'$, which is physically unaceptable. Thus, at least for zirconium and Zircaloy-4, Shvedov's model is not applicable. Furthermore, it can be stated in general that in the comparison between the theory and the experiments there are too many adjustable parameters. In any case, it is clear that the activation enthalpy obtained from the internal friction peak has a physical meaning only within a specific model.

The exact meaning of the viscosity coefficient for grain-boundary sliding will become clear only in the framework of a detailed atomistic model of the grain boundary. Ashby [21], for example, has calculated the viscosity coefficient when grain-boundary sliding does not occur in a continuous way, but discontinously, by the motion of appropriate dislocations in the boundary plane. For a tilt boundary of angle θ in a square lattice he obtained

$$\eta = kT/8bD_b(\varrho L) \quad (28)$$

where ϱ is the linear density of dislocations in the boundary, L is the translation periodicity in the boundary and b is the atomic size. Equation 28 reduces to

$$\eta = kT/8bD_b \quad (29)$$

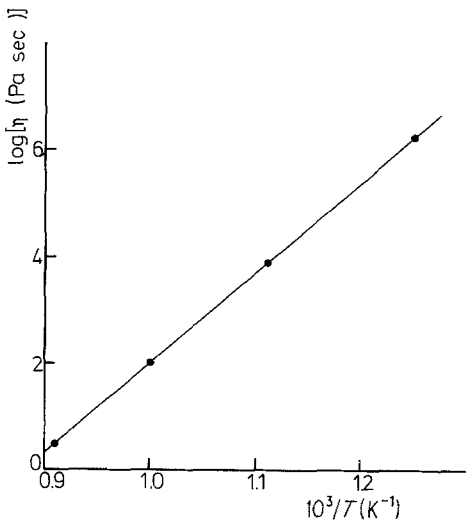

Figure 7 Viscosity coefficient associated with grain-boundary sliding against the reciprocal of temperature, for Zircaloy-4.

when $\varrho = 1/L$. According to Ashby [21], Equation 29 gives a lower bound for the viscosity of a symmetric tilt boundary. On comparing Equation 10 with Equations 28 and 29 it is seen that η depends on the thickness of the boundary, in the first case, contrary to Equations 28 and 29 where η does not depend on d. Fig. 7 shows the temperature dependence of η calculated with Equation 10 and $a = d = b$, where b is the lattice parameter for zirconium and D_b given by Equation 25. A straight line with the same slope and lower intercept, due to the factor 1/8, will be obtained with Equation 29.

5. Conclusions

The two internal friction peaks present on the HTIF of Zircaloy-4 can be interpreted in terms of relaxation mechanisms occurring at the grain boundaries. The lowest-temperature peak is produced by the sliding of particle-free boundaries and the peak occurring at higher temperatures has been associated with the sliding of particle-bearing boundaries. Similar mechanisms were also proposed for the HTIF of zirconium.

The characteristics of both peaks have been measured in detail and both the diffusion coefficient and the activation enthalpy for diffusion along grain boundaries have been obtained from the internal friction data.

Finally, the viscosity coefficient associated with grain-boundary sliding was determined as a function of temperature.

Acknowledgements

This work was supported in part by the German–Argentine Cooperation Agreement in Scientific Research and Technological Development, by the CIC and by the Proyecto Multinacional de Tecnología de Materiales, OAS-CNEA.

Appendix A

According to Equations 5, 7 and 8, Q^{-1} reaches a maximum at

$$C = 4.269$$
$$p = 1.4719$$
$$q = 0.393 \quad (A1)$$

and the C, p and q values at half maximum are

$$C_1 = 1.4367 \quad C_2 = 6.070$$
$$p_1 = 0.375 \quad p_2 = 12.954$$
$$q_1 = 0.3277 \quad q_2 = 0.4782 \qquad \text{(A2)}$$

Taking the logarithm of Equation 12 leads to

$$\ln C = \ln \frac{2\pi^2(1 - \nu) lfk}{ab D_{b0} \mu} + \ln T + \frac{\Delta H_b}{kT} \qquad \text{(A3)}$$

which on taking increments and rearranging gives

$$\Delta(T^{-1}) = (\Delta \ln C - \Delta \ln T) k/\Delta H_b \qquad \text{(A4)}$$

This equation can be used to calculate the peak width at half maximum when the internal friction is measured as a function of temperature. In fact, from Equation A2

$$\Delta \ln C = \ln(C_2/C_1) = 2.199 \qquad \text{(A5)}$$

so that

$$\Delta(T^{-1}) = (2.199 - \Delta \ln T) k/\Delta H_b \qquad \text{(A6)}$$

In general $\Delta \ln T \ll 2.199$ and Equation A6 reduces to

$$\Delta(T^{-1}) = 2.199 k/\Delta H_b \qquad \text{(A7)}$$

The corresponding width at half maximum for a Debye-type peak is [6]

$$\Delta(T^{-1}) = 2.635 k/\Delta H \qquad \text{(A8)}$$

On comparing Equations A7 and A8 it is seen that Equation 5 predicts an internal friction peak slightly narrower than a Debye peak. Furthermore, the internal friction peak described by Equation 5 can be compared with a Debye peak with the same relaxation strength, i.e.

$$Q^{-1} = 0.293\pi(1 - \nu) \frac{\omega\tau}{1 + \omega^2\tau^2} \qquad \text{(A9)}$$

by introducing

$$\tau = [\pi(1 - \nu) l/4.269 \mu d] \eta \qquad \text{(A10)}$$

The Debye peak given by Equation A9 and the peak described by Equation 5 are compared in Fig. 5.

Appendix B

An estimation of the concentration of impurities needed to saturate the grain boundaries can be made for a specimen of given dimensions. In fact, in a specimen of radius r and length L, with cubic grains of size l and width d, the volume to be filled with impurities is

$$V_i \cong (3nl^2 - 2\pi rL - 2\pi r^2) d \qquad l \gg d \qquad \text{(B1)}$$

and the numbers of impurity atoms, n_i, is

$$n_i = \frac{d}{\Omega}(3nl^2 - 2\pi rL - 2\pi r^2) \qquad \text{(B2)}$$

where n in the number of grains in the specimen and Ω is the atomic volume. But

$$n = \pi r^2 L/(l + d)^3 \qquad \text{(B3)}$$

and substituting Equation B3 into Equation B2 leads to

$$n_i = \frac{2\pi rLd}{\Omega}\left(\frac{3rl^2}{2(l + d)^3} - 1 - \frac{r}{L}\right) \qquad \text{(B4)}$$

By definition, the atomic concentration of impurities is given by

$$c = n_i/(n_i + n_a) \simeq n_i/n_a \qquad \text{(B5)}$$

where

$$n_a = \varrho\pi r^2 L N_A/\omega \qquad \text{(B6)}$$

is the number of solvent atoms. ϱ is the density of the material, ω is the atomic weight of the solvent atoms and N_A is Avogadro's number. On substituting Equations B4 and B6 into Equation B5 and taking into account that $l \gg d$, this leads to

$$c = \frac{d\omega}{\Omega\varrho N_A}\left(\frac{3}{l} - \frac{2}{r} - \frac{2}{L}\right) \qquad \text{(B7)}$$

Usually, l is much smaller than r and L and Equation B7 reduces to

$$c \simeq (3d\omega/\Omega\varrho N_A l) \qquad \text{(B8)}$$

For the particular case of the specimens considered in the paper $l = 30\,\mu$m, $\varrho(\text{Zr}) = 6.506\,\text{g cm}^{-3}$, $\omega(\text{Zr}) = 91.22\,$g and on taking $\Omega = b^3$ and $d = b$, where b is the lattice parameter of zirconium (3.23×10^{-10}m), Equation B8 gives $c = 2.2 \times 10^{-5}$.

References

1. F. POVOLO and B. J. MOLINAS, *J. Nucl. Mater.* **114** (1983) 85.
2. J. L. GACOUGNOLLE, S. SARRAZIN and J. de FOUQUET, *J. Physique* **32** (1971) C2-21.
3. K. BUNGARDT and H. PREISENDANZ, *Z. Metallkde* **51** (1960) 280.
4. F. POVOLO, A. F. ARMAS and B. J. MOLINAS, *J. Phys. E* **17** (1984) 121.
5. F. POVOLO and B. J. MOLINAS, in "Strength of Metals and Alloys", Vol. 1, edited by R. C. Gifkins (Pergamon Press, Oxford, 1983) p. 89.
6. A. S. NOWICK and B. S. BERRY, "Anelastic Relaxation in Crystalline Solids" (Academic Press, New York, 1972) pp. 58, 94.
7. I. G. RITCHIE and K. W. SPRUNGMANN, Atomic Energy of Canada Ltd. Report AECL-6810 (Pinawa, 1981).
8. F. POVOLO and B. J. MOLINAS, *J. Mater. Sci.* **20** (1985) 3649.
9. Z. Q. SUN and T. S. KÊ, *J. Physique* **42** (1981) C5-451.
10. H. E. ROSINGER, I. G. RITCHIE and A. J. SHILLINGLAW, Atomic Energy of Canada Ltd. Report AECL-5231 (Pinawa 1975).
11. F. POVOLO and R. E. BOLMARO, *J. Nucl. Mater.* **118** (1983) 78.
12. F. SCHÜCKNER, in "Quantitative Microscopy", edited by R. T. DeHoff and F. N. Rhines (McGraw-Hill, New York, 1968) p. 201.

13. J. C. COLIN and P. LEHR, in Proceedings of IX^{e} Colloque de Métallurgie, Centre d'Etudes Nucléaires de Saclay, June 1965 (Presse Universitaires de France, 1966) p. 77.
14. A. S. NOWICK and B. S. BERRY, *IBM J.* **5** (1961) 297.
15. T. MORI, M. KODA, R. MONZEN and T. MURA, *Acta Metall.* **31** (1983) 275.
16. F. POVOLO and A. J. MARZOCCA, *J. Nucl. Mater.* **118** (1983) 224.
17. *Idem, ibid.* **119** (1983) 78.
18. H. GLEITER and B. CHALMERS, in "Progress in Materials Science", Vol. 16 (Pergamon Press, Oxford, 1972) p. 98.
19. D. R. MOSHER and R. RAJ, *Acta Metall.* **22** (1974) 1469.
20. Y. A. SHVEDOV, *Scripta Metall.* **13** (1979) 801.
21. M. F. ASHBY, *Surf. Sci.* **31** (1972) 498.

Received 9 July 1984
and accepted 19 December 1985